Supplementary Information

Conducting polymer/hydrogel hybrid free-standing electrodes for flexible supercapacitors capable of self-sensing working conditions: large-scale fabrication through facile and low-cost route

Madari Palliyalil Sidheekha[a], Aranhikundan Shabeeba[a], Lijin Rajan[a], Mohamed Shahin Thayyil[b], Yahya A. Ismail[a]*

[a] *Advanced Materials Research Center, Department of Chemistry, University of Calicut, Thenhipalam, Kerala - 673635, India*

[b] *Department of Physics, University of Calicut, Thenhipalam, Kerala - 673635, India*

***Correspondence**

Yahya A. Ismail

Department Of Chemistry, University of Calicut, Kerala, India- 673635

aiyahya@uoc.ac.in

1. Cs/PANI hybrid film

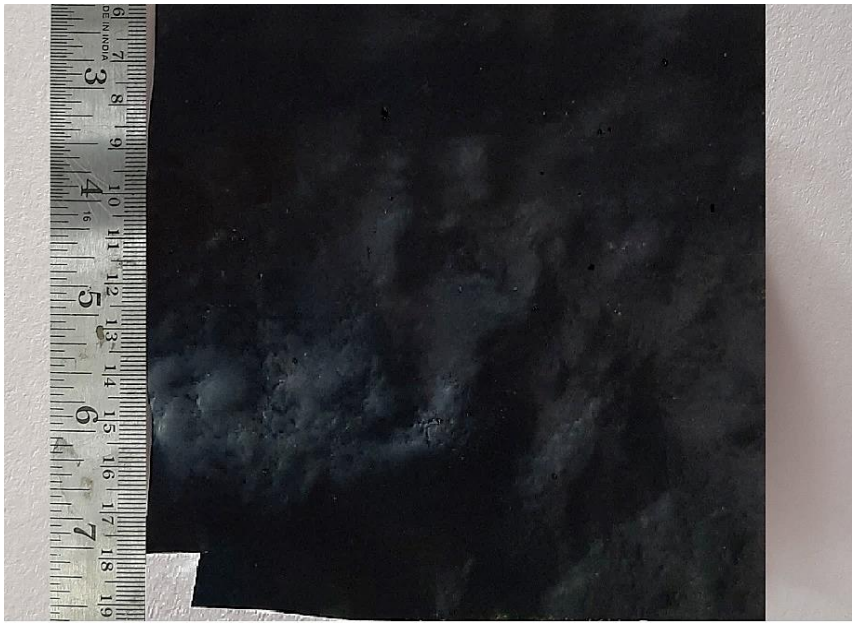

Fig. S1: photograph of fabricated CPF hybrid hygrogel film

2. EDS analysis

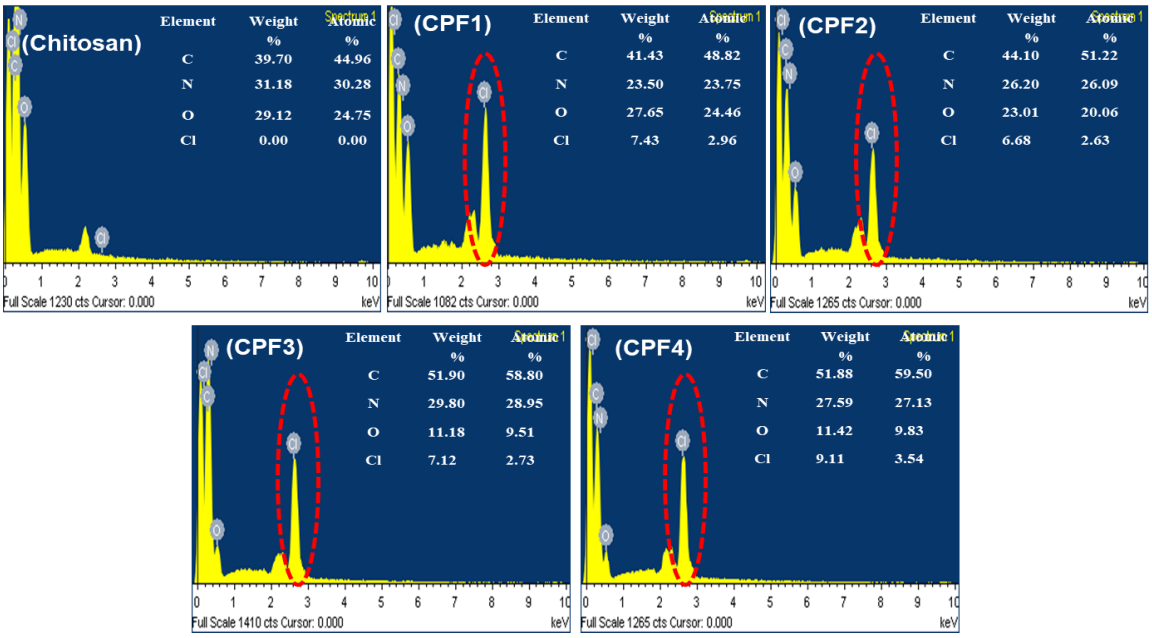

Fig. S2: SEM-EDX spectra of Chitosan and CPF films

3. Cyclic voltammograms at different scan rate

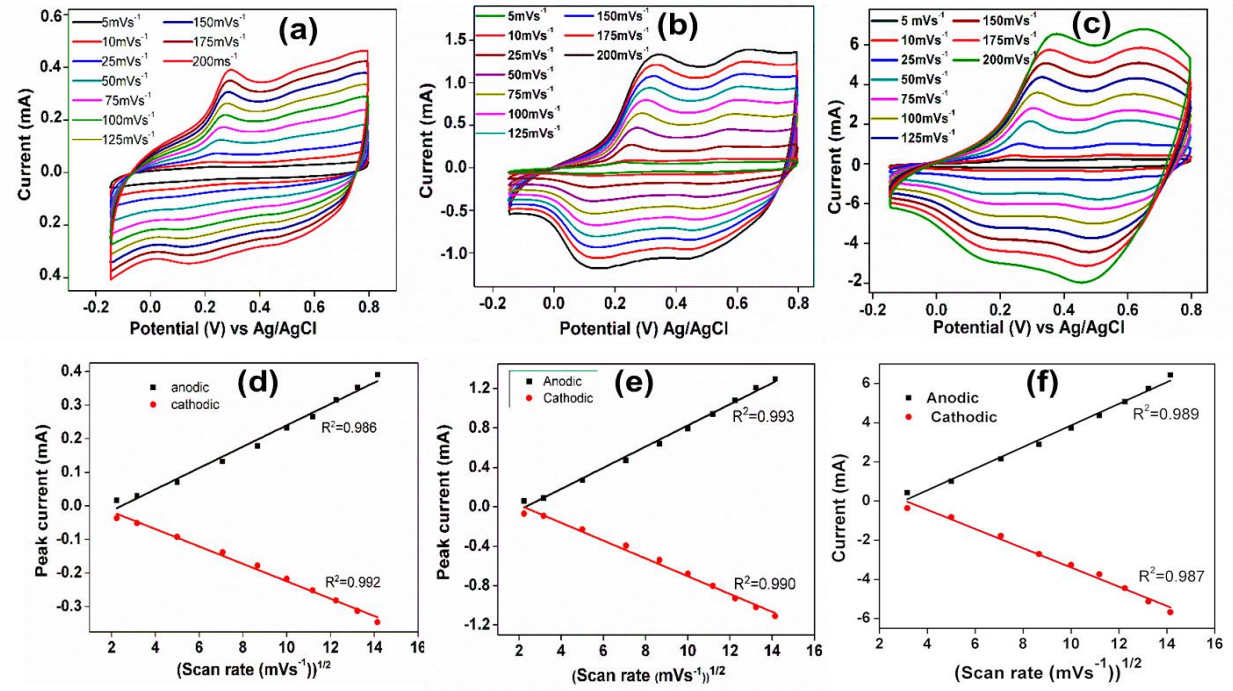

Fig. S3: (a,b and c) CVs obtained at different scan rates for CPF1, CPF2 and CPF3 films respectively and (c,d and f) variation peak current as a function of square root of scan rate for CPF1, CPF2 and CPF3 films respectively

4. Chronopotentimetric responses during consecutive oxidation/reduction cycles

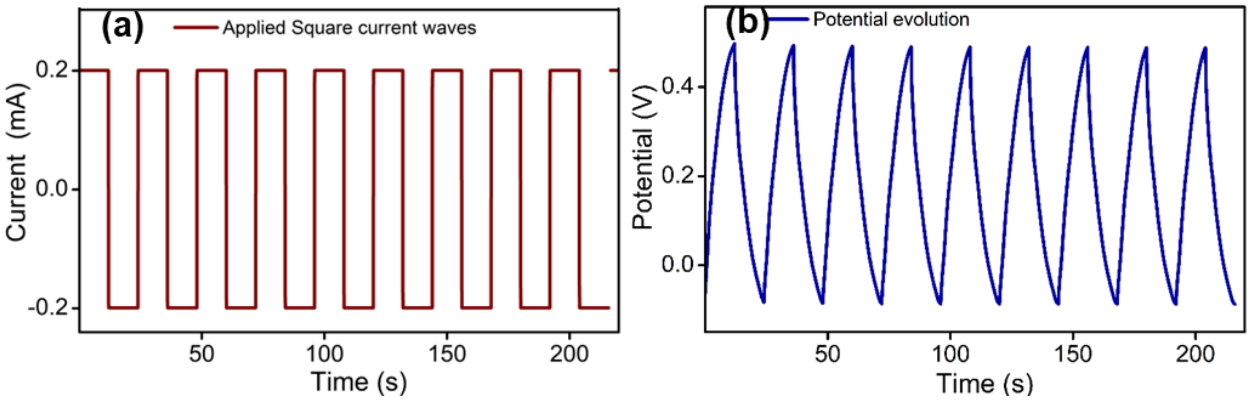

Fig. S4: (a) A representative square current waves applied to the CPF working electrode and (b) resulting chronopotentiometric responses

5. CVs of CPF films at the scan rate of 5 mV s^{-1}

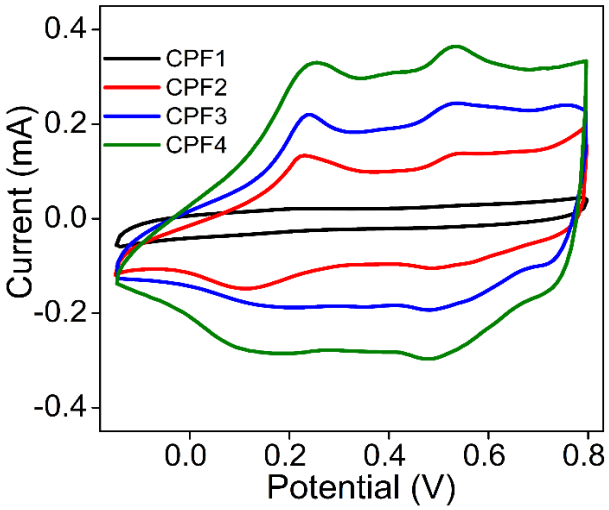

Fig. S5: CVs at scam rate of 5 mV s^{-1}

6. Chronopotentiogram at different working current at constant charge for the device

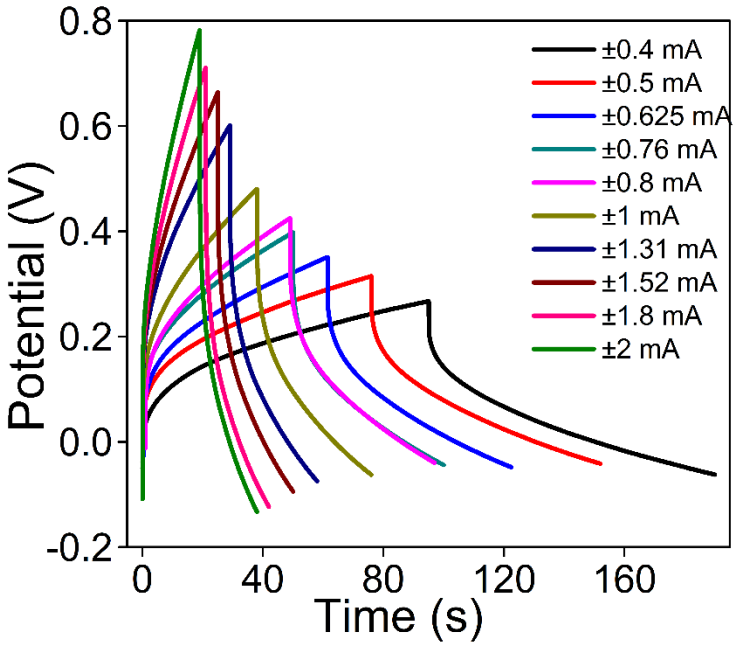

Fig. S6: Normalized second cycle of charge-discharge (oxidation-reduction) curve at different working (charging/discharging) currents by consuming constant charge of ±38 mC

7. Mechanical properties of CPF films

Table S1: Tensile strength, Young's Modulus and % elongation at break of CPF films

Film	Tensile strength (MPa)	Young's Modulus (MPa)	% Elongation at break
CPF1	9.82	2.32	8.12
CPF2	8.22	1.99	7.08
CPF3	6.64	1.85	6.42
CPF4	5.84	1.56	5.86

8. CV peaks of CPF film at scan rate 25 mV/s

Table S2: Anodic and cathodic peaks of CPF electrodes at the scan rate 25 mV/s

Film	Anodic peaks (V)		Cathodic peaks (V)	
	LE to ES	ES to PN	PN to ES	ES to LE
CPF1	0.27	0.54	0.43	0.059
CPF2	0.28	0.54	0.42	0.11
CPF3	0.28	0.59	0.48	0.19
CPF4	0.29	0.57	0.45	0.13

LE- leucoemeraldine, ES- emeraldine salt, PN- pernigraniline

9. Comparison of CPF supercapacitor with other PANI- hydrogel-based supercapacitors reported in the literature.

Table S3: Comparison of CPF supercapacitor with other PANI- hydrogel-based supercapacitors reported in the literature.

Type of electrode	Areal capacitance	Separator/ electrolyte	Maximum energy density @ Power density	Ref.
Chitosan/PANI	111 mF cm^{-2} @ 0.4 mA cm^{-2} 222 mF cm^{-2} @ 5mV/s	PVA/H_2SO_4	13.8 µWh cm^{-2} @ 100 µW cm^{-2}	*This work*
Graphene / PANI	23 mF cm^{-2} @ 0.1 mA cm^{-2}	PVA/H_3PO_4	1.5 µWh cm^{-2} @ 330 µW cm^{-2}	[1]
CNFs/PANI/rGO	5.86 mF cm^{-2} @ 4.3 µA cm^{-2}	PVA/H_2SO_4		[2]
CNFs/[PANI–PEDOT: PSS]	4.22 mF cm^{-2} @ 4.3 µA cm^{-2}	PVA/H_2SO_4		[2]
PVA /PANI	25.86 mF cm^{-2} @ 0.05 mA cm^{-2}	PVA/H_2SO_4		[3]
PANI/PVA/PHEA	98 mF cm^{-2} @ 0.2 mA cm^{-2}	PVA/PHEA/ H_2SO_4	8.48 µWh cm^{-2} @ 78.52 µW cm^{-2}	[4]
SWCNT/PANI/ PVA	15.8 mF cm^{-2} @0.044 mA cm^{-2}	PVA/H_2SO_4		[5]
rGO/PANI	6.4 mF cm^{-2} @ 0.08 mA cm^{-2}	PVA/H_2SO_4	7.07 Wh kg^{-1} @ 707 W kg^{-1}	[6]
Fe^{3+}/ PANI/Cellulose	185 mF cm^{-2} @ 0.2 mA cm^{-2}	H_2SO_4	~ 6.2 µWh cm^{-2} @ ~110 µW cm^{-2}	[7]
PHE/PANI	131 mF cm^{-2} @ 0.2 mA cm^{-2}	PHE/H_3PO_4	11.6 µWh cm^{-2} @ 79.9 µW cm^{-2}	[8]
Graphite/PANI	77.8 mF cm^{-2} @ 0.1 mA cm^{-2}	PVA/H_2SO_4	0.32 mWh cm^{-3} @ 0.054 W cm^{-3}	[9]

NiO/Graphene/ PANI	112 mF cm^{-2} @ 2 mV s^{-1}	cellulose/ KOH		[10]
PVA/PANI	11.3 mF cm^{-2} @ 5 mVs^{-1}	PVA/H_2SO_4		[11]
rGO/PANI-CH_4	45 mF cm^{-2} @ 0.2 mA cm^{-2}	PVA/H_2SO_4		[12]
CNT/PANI	38 mF cm^{-2} @ 0.01 mA cm^{-2}	PVA/H_2SO_4		[13]
CNF/CNTs/PANI	67.31 mF cm2 @ 0.5 mA cm^{-2}	PVA/H_3PO_4		[14]
Graphene/sulfonated PANI	3.31 mF cm^{-2} @ 10 mV s^{-1}	PVA/H_2SO_4	1.51 mWh cm^{-3}	[15]
Cellulose /PAA/PANI	1.73 mF cm^{-2} @ 5 mV s^{-1}	H_2SO_4	0.62 µWh cm^{-2} @ 7.03 µW cm^{-2}	[16]
PANI/PLA(Symmetric)	0.20 mF cm^{-2} @ 4 µA cm^{-2}	PVA/H_2SO_4	3.60 µWh cm^{-2} @ 0.02 µW cm^{-2}	[17]
PANI/PLA(Asymmetric)	23.33 mF cm^{-2} @0.05 $mAcm^{-2}$	PVA/H_2SO_4	30.09 µWcm^{-2} @ 1.17µWh cm^{-2}	[17]
PANI- foamed PLA	27.73 mF cm^{-2} @ 0.05 mA cm^{-2}	PVA/H_2SO_4	1.89 µWh cm^{-2} @ 35 µWh cm^{-2}	[18]
PANI−Stainless Steel wire	~19 mF cm^{-2} @ 0.1 mA cm^{-2}	H_2SO_4	0.95 µWh cm^{-2} @ ~100 µW cm^{-2}	[19]

CNFs- Cellulose nanofiber; rGO- reduced graphene oxide; PHEA- poly (N-hydroxyethyl acrylamide); SWCNT- single-walled carbon nanotube; PHE- polymer hydrogel electrolyte (polyacrylic acid crosslinked with vinyl hybrid silica nanoparticles); CNT- carbon nanotube; PAA- polyacrylic acid; PLA- polylactic acid.

10. EIS Fitting data of device

Table S4: The best fitting values of the equivalent circuit elements in Figure 13e for the impedance data of CPF device

Parameters	**Rs** (Ω)	**R_{ct1}** (Ω)	**Q_1 (CPE_1)** ($S \cdot s^{\alpha 1}$)	**α_1**	**R_{ct2}** (Ω)	**Q_2 (CPE_2)** ($S \cdot s^{\alpha 2}$)	**α_2**	**Q_3 (CPE_3)** ($S \cdot s^{\alpha 2}$)	**α_3**
Before cycling stability test									
Circuit values	13.4	0.50	0.12	1.22	5.3	0.051	0.82	0.0082	0.56
After cycling stability test									
Circuit values	14.4	0..26	0.08	1.12	14.0	0.017	0.90	0.012	0.51

References

[1] X. Zang, X. Li, M. Zhu, X. Li, Z. Zhen, Y. He, K. Wang, J. Wei, F. Kang, H. Zhu, 2015, **7**, 7318-7322. https://doi.org/10.1039/C5NR00584A

[2] X. Wang, K. Gao, Z. Shao, X. Peng, X. Wu, F. Wang, *J. Power Sources*, 2014, **249**, 148-155. https://doi.org/10.1016/j.jpowsour.2013.09.130

[3] W. Li, X. Li, X. Zhang, J. Wu, X. Tian, M.-J. Zeng, J. Qu, Z.-Z. Yu, *ACS Appl. Energy Mater.*, 2020, **3**, 9408-9416. https://doi.org/10.1021/acsaem.0c01794

[4] J. Yang, X. Yu, X. Sun, Q. Kang, L. Zhu, G. Qin, A. Zhou, G. Sun, Q. Chen, *ACS Appl. Mater. Interfaces*, 2020, **12**, 9736-9745. https://doi.org/10.1021/acsami.9b20573

[5] Y. Guo, K. Zheng, P. Wan, *Small*, 2018, **14**, 1704497. https://doi.org/10.1002/smll.201704497

[6] F. Chen, P. Wan, H. Xu, X. Sun, *ACS Appl. Mater. Interfaces*, 2017, **9**, 17865-17871. https://doi.org/10.1021/acsami.7b02460

[7] Z. Liu, J. Chen, Y. Zhan, B. Liu, C. Xiong, Q. Yang, G.-H. Hu, *ACS Sustain. Chem. Eng.*, 2019, 7, 17653-17660. https://doi.org/10.1021/acssuschemeng.9b03674

[8] R. Jia, H. Du, X. Zhang, Z. Chen, D. Chen, *J. Electrochem. Soc.*, 2018, **165,** A3792. https://doi.org/10.1149/2.0481816jes

[9] B. Yao, L. Yuan, X. Xiao, J. Zhang, Y. Qi, J. Zhou, J. Zhou, B. Hu, W. Chen, *Nano Energy*, 201, **2**, 1071-1078. https://doi.org/10.1016/j.nanoen.2013.09.002

[10] X. Wu, Q. Wang, W. Zhang, Y. Wang, W. Chen, Electrochim. Acta, 2016, **211**, 1066-1075. https://doi.org/10.1016/j.electacta.2016.06.026

[11] R. Hu, J. Zhao, R. Jiang, J. Zheng, *J. Mater. Sci.: Mater. Electron.*, 2017, **28**, 14568-14574. https://doi.org/10.1007/s10854-017-7320-9

[12] K. Wang, B. Zheng, M. Shrestha, T. Schuelke, Q.-H. Fan, *Energy Stor. Mater.*, 2018, **14**, 230-237. https://doi.org/10.1016/j.ensm.2018.04.004

[13] K. Wang, Q. Meng, Y. Zhang, Z. Wei, M. Miao, *Adv. Mater.*, 2013, **25**, 1494-1498. https://doi.org/10.1002/adma.201204598

[14] J.-h. Liu, X.-y. Xu, W. Lu, X. Xiong, X. Ouyang, C. Zhao, F. Wang, S.-y. Qin, J.-l. Hong, J.-n. Tang, Electrochim. Acta, 2018, **283**, 366-373. https://doi.org/10.1016/j.electacta.2018.06.158

[15] B. Song, L. Li, Z. Lin, Z.-K. Wu, K.-s. Moon, C.-P. Wong, *Nano Energy*, 2015, **16**, 470-478. https://doi.org/10.1016/j.nanoen.2015.06.020

[16] S. Ke, Z. Wang, K. Zhang, F. Cheng, J. Sun, N. Wang, Y. Zhu, *Polymers*, 2020, **12**, 1369. https://doi.org/10.3390/polym12061369

[17] W. Huige, L. Guixing, W. Tong, C. Anli, P. Zifang, H. Zhang, 复合材料学报, **39**, 2022, 193-202. https://doi.org/10.13801/j.cnki.fhclxb.20210517.001

[18] G. Li, L. Wang, X. Lei, Z. Peng, T. Wan, S. Maganti, M. Huang, V. Murugadoss, I. Seok, Q. Jiang, *Adv. Compos. Hybrid Mater*., 2022, **6**,1-11. https://doi.org/10.1007/s42114-022-00501-7

[19] Y. Fu, H. Wu, S. Ye, X. Cai, X. Yu, S. Hou, H. Kafafy, D. Zou, *Energy Environ. Sci*., 2013, **6**, 805-812. https://doi.org/10.1039/C3EE23970E